Catalysis Science & Technology

Computational and Experimental Investigation of Co and S-doped Ni2P as Efficient Electrocatalyst for Acid Mediated Proton Exchange Membrane Hydrogen Evolution Reaction

Journal:	*Catalysis Science & Technology*
Manuscript ID	CY-ART-09-2020-001862.R1
Article Type:	Paper
Date Submitted by the Author:	01-Nov-2020
Complete List of Authors:	Ghadge, Shrinath; University of Pittsburgh, Chemical and Petroleum Engineering Velikokhatnyi, Oleg; University of Pittsburgh, Bioengineering Datta, Monikanchan; University of Pittsburgh, Bioengineering Shanti, Pavithra; university of pittsburgh Kumta, Prashant; University of Pittsburgh, Department of BioEngineering

Manuscript ID: CY-ART-09-2020-001862

Computational and Experimental Investigation of Co and S-doped Ni_2P as Efficient Electrocatalyst for Acid Mediated Proton Exchange Membrane Hydrogen Evolution Reaction

Shrinath Dattatray Ghadge[a], Oleg I. Velikokhatnyi[b,c], Moni K. Datta[b,c], Pavithra M. Shanthi[a], and Prashant N. Kumta[a,b,c,d,e *]

[a] Chemical and Petroleum Engineering, Swanson School of Engineering, University of Pittsburgh, PA 15261

[b] Department of Bioengineering, Swanson School of Engineering, University of Pittsburgh, PA 15261

[c] Center for Complex Engineered Multifunctional Materials, University of Pittsburgh, PA 15261

[d] Mechanical Engineering and Materials Science, University of Pittsburgh, Pittsburgh, PA 15261

[e] School of Dental Medicine, University of Pittsburgh, PA 15217

[*]Corresponding author: pkumta@pitt.edu

Abstract

Engineering earth-abundant and high performance electrocatalysts to facilitate hydrogen evolution reaction (HER) for generation of sustainable hydrogen fuel has been a major scientific and technological challenge in the electrolytic water splitting area. Herein, employing theoretical first principles calculations of HER thermodynamics and kinetics-based density functional theory (DFT), we report a platinum group metal (PGM)-free Co and S containing Ni_2P [$(Ni_{0.95}Co_{0.05})_2P$:x at. % S (x = 5, 10, 15)] system as highly active and robust electrocatalysts for acidic HER. On the basis of the DFT calculations, $(Ni_{0.95}Co_{0.05})_2P$:15S composition reveals optimal hydrogen adsorption free energies (ΔG_{H^*}) and beneficial modification of the surface electronic structure. Accordingly, $(Ni_{0.95}Co_{0.05})_2P$:15S electrocatalyst, synthesized via a simple and facile low temperature solid state approach, demonstrates significantly higher HER performance in comparison to pristine Ni_2P and comparable HER performance to state-of-the-art Pt/C. Owing to the unique modification of the electronic structure i.e. change in density of state (DOS) and optimized ΔG_{H^*}, the $(Ni_{0.95}Co_{0.05})_2P$:15S composition exhibits considerably lower charge transfer resistance (6.82 Ω cm^2), lower over-potential (44 mV at 10 mA cm^{-2}), smaller Tafel slope (31.25 mV dec^{-1}), smaller water contact angle (7^o) and correspondingly, a smaller bubble break-off diameter (0.38 mm) with a higher mass activity (43.75 A g^{-1} at -0.05 V) in comparison to $(Ni_{0.95}Co_{0.05})_2P$:x at.% S (x = 0, 5, 10) and Ni_2P. The highly active composition, $(Ni_{0.95}Co_{0.05})_2P$:15S also displays a long term electrochemical HER stability, similar to Pt/C, with no major degradation in the activity, reflective of its excellent structural robustness for acidic HER.

Consequently, the present experimental study fortified by theory provides novel synergistic insights into designing promising and efficient multi-component HER electrocatalysts.

Keywords: earth-abundant, platinum group metal free, hydrogen evolution reaction, hydrogen adsorption free energies, electrocatalyst

[Note: The present work has been presented at the Electrochemical Society biannual meeting-PRiME 2020, October 4-9, 2020]

1. Introduction

Hydrogen (H_2), a non-carbonaceous fuel with higher energy density (~120 MJ/kg) than the fossil fuels based conventional energy sources (~45 MJ/kg) is considered as one of the most promising and sustainable energy carriers.[1-4] Among the various hydrogen production technologies such as coal gasification and steam reforming, hydrogen generation via electrocatalytically water splitting involving cathodic hydrogen evolution reaction (HER) and anodic oxygen evolution reaction (OER) constitutes one of the most environmentally friendly, clean, and reliable approaches, devoid of any substantial carbon footprints.[5-7] Owing to their significant electrocatalytic activity with minimum overpotential and adequate electrochemical durability, various state-of-the-art platinum group metal (PGM) based electrocatalysts such as Pt, IrO_2, RuO_2, etc. are commonly utilized as OER and HER electrocatalysts in electrochemical water splitting. However, the prohibitive cost (~\$210,000/kg_{Pt}) and scarcity of global reserves (~0.001-

0.005 ppm in earth's crust) of PGM electrocatalysts represent major bottlenecks thwarting the progress towards their large-scale utilization in operation of water electrolyzers. [8, 9]

The identification, synthesis, and improvement of earth-abundant, cost-efficient, and PGM-free electrocatalysts, exhibiting comparable/superior electrochemical performance in comparison to the state-of-the art and expensive electrocatalysts to expedite the HER-OER kinetics is therefore an integral and principal research objective of researchers engaged in the electrocatalysis arena. In relation to HER, numerous transition-metal (e.g. Fe, Cu, Ni, Co) phosphides (TMPs), sulfides, carbides, selenides, nitrides, etc. have been explored for the more advantageous proton exchange membrane (PEM) based acidic hydrogen evolution. [10-12] Amongst these systems, TMPs, owing to their excellent hydrodesulfurization (HDS) characteristics which rely on reversible binding of hydrogen on the catalyst surface, similar to HER, are highly promising and widely studied HER electrocatalyst systems.[13] In recent years, therefore, various TMPs such as copper phosphides, nickel phosphide, iron phosphides, molybdenum phosphides, tungsten phosphides, etc. have been studied as an active HER electrocatalysts.[3, 14] Among these TMP systems, Ni_2P has been reported to be a highly promising HER electrocatalyst owing to the presence of (i) a weak "ligand effect" due to Ni-P bonds, expediting the dissociation of molecular H_2, (ii) the "ensemble effect" of P which decreases the number of active sites on the surface preventing the poisonous effects due to high coverage, and (iii) presence of P sites providing an adequate bonding strength to the evolved H_2 molecule.[13, 15] Nevertheless, despite demonstrating noticeable HER performance, pristine Ni_2P suffers from a larger overpotential (>150 mV) and thus, lower HER performance in the stringent acidic electrolytes in comparison to the characteristic HER performance of benchmark, state-of-the-art Pt/C electrocatalyst.

In the present study, correspondingly, in order to engineer non-PGM HER electrocatalysts exhibiting excellent electrocatalytic activity, durability, and optimized electronic structure, compatible to that of Pt/C electrocatalyst, we have executed theoretical first-principles electronic structure calculations involving determination of the hydrogen binding energy (ΔG_{H^*}) to the surface of electrocatalysts. Correspondingly, we have identified cobalt (Co) and sulphur (S) incorporated Ni_2P, denoted as $(Ni_{0.95}Co_{0.05})_2P$: x at. % S (x = 5, 10, 15) as high performance HER electrocatalyst systems, for very first time to the best of our knowledge. There are various electrocatalyst development strategies and introduction of heteroatom into the parent electrocatalyst (herein Ni_2P) is one of the most utilized approaches to modulate the electronic structure, consequently, altering the electrocatalytic activity.

The as-performed density functional theory (DFT) calculations conducted in the present work reveal that the synergistic effect of incorporating Co and S into Ni_2P can beneficially modify the electronic structure and d-band of bimetallic phosphosulphide [$(Ni_{0.95}Co_{0.05})_2P$: S], resulting in the hydrogen adsorption free energy (ΔG_{H^*}) shifting towards the thermoneutral position.[16] In the present study, the rationale for selecting Co and S as dopant atoms is their ability to offer the promotional effect i.e. lowering the charge transfer resistance (R_{ct}), improving the electronic conductivity, and thus, enhancing the HER

performance as evidently reported in the various HER, OER as well as HDS based electrocatalyst studies.[3] Based on the theoretical results predicting the optimized surface electronic structure for HER, we have devised a synthetic strategy to fabricate the solid solution of $(Ni_{0.95}Co_{0.05})_2P$: x at. % S (x = 5, 10, 15) compositions via a simple, economical, and facile solid-state synthesis approach. Relying on the beneficial synergistic effect of Co and S incorporation, the as-prepared $(Ni_{0.95}Co_{0.05})_2P$:15S electrocatalyst exhibits a high electrocatalytic performance towards acidic HER with the optimized ΔG_{H^*}, cohesive energy (E_{coh}), significantly lower overpotential, excellent HER activity and durability, comparable to Pt/C. The present work therefore putatively, documents the simultaneous incorporation of Co and S into the Ni_2P lattice, offering a promising opportunity for tailoring the physical, electronic, and electrocatalytic properties of bimetallic phosphosulphide to match the Pt/C based HER system.

2. Computational Methodology

The electrocatalytic activity of HER electrocatalyst can be described by a single parameter ΔG_{H^*}, which is the free energy of adsorbed hydrogen atom on the

electrocatalytic surface. The low value of ΔG_{H^*} (i.e. close to zero) indicates the more optimal adsorption and desorption of hydrogen species at the electrocatalyst surface and thus, offering higher overall electrocatalytic activity of the electrocatalyst material.[17-19] In general, ΔG_{H^*} is represented by the following relation: $\Delta G_{H^*} = \Delta E_{H^*} + \Delta ZPE - T\Delta S$, where the reaction energy ΔE_{H^*} is calculated using the DFT based methodology as shown below:

$$\Delta E_{H^*} = E(slab + nH) - E(slab + (n-1)\,H) - 1/2\,E(H_2). \quad \textbf{(eq. 1)}$$

Here, E(slab + nH) is the total energy of a catalyst surface slab with n hydrogen atoms adsorbed on the surface, E(slab + (n-1)H) is the total energy of the corresponding catalyst surface slab with (n-1) hydrogen atoms (after removal of one hydrogen atom from the given site), and $E(H_2)$ is the total energy of the hydrogen molecule in the gas phase. Also, for calculations of ΔG_{H^*} for all the electrocatalyst materials, the zero point energy correction ΔZPE minus the entropy term $T\Delta S$ ($\Delta ZPE - T\Delta S$) has been taken as 0.24 eV, following the computational study by Nørskov et al.[19]

For calculations of the bulk and surface properties of Ni_2P:S, a hexagonal crystal structure P-62m (space group #189) with three formula units in the unit cell and the lattice

parameters $a = b = 5.859$Å and $c = 3.382$Å have been considered as shown in **Figure 1a**.[20, 21] In all the calculations, one monolayer of H-coverage on the (0001) surface has been considered. There are two terminations of (0001) surfaces of Ni_2P structure, namely Ni_3P and Ni_3P_2. Previous DFT study conducted by Q. Li and X. Hu showed that the (0001) surface prefers Ni_3P_2 terminations due to higher stability.[22] Thus, this surface termination has been chosen with triple-Ni sites considered being catalytically active (**Figure 1a)** for the present DFT study of hydrogen binding energies as a qualitative descriptor of the HER catalytic activity (**eq. 1**).

The common surface slab used in the present DFT study consists of five atomic layers corresponding to two lattice parameters in the *c* direction which is perpendicular to (0001) crystallographic plane and separated by vacuum layer of ~20 Å to prevent the interaction between the slab and its image. The first two layers are fixed with bulk structural parameters, while the remaining three top layers were allowed to relax together with all the adsorbed hydrogen atoms on the surface. Herein, since the purpose of the present theoretical study is to illuminate the effects of introduction of Co and S elements on the overall electrocatalytic activity of Ni_2P, thus, only one composition of each dopant has been selected for the calculation of ΔG_{H^*} and other properties of the corresponding compounds. Therefore the ΔG_{H^*} values been calculated for pure Ni_2P, $(Co_{0.17}Ni_{0.83})_2P$, and $(Co_{0.17}Ni_{0.83})_2P_{0.67}$:$S_{0.33}$

compositions. Further details of the computational methodology are given in Supplementary Information.

3. Experimental methodology

3.1 Synthesis of $(Ni_{0.95}Co_{0.05})_2P$:x at.% S (x= 0, 5, 10, 15) nanoparticles (NPs)

Schematic illustration of the various steps involved in the synthesis of $(Ni_{0.95}Co_{0.05})_2P$:S electrocatalyst is outlaid in **Figure 2**. Specifically, Nickel (II) chloride hexahydrate ($NiCl_2.6H_2O$, 98%, Acros Organics), cobalt chloride hexahydrate ($CoCl_2.6H_2O$, 98%, Aldrich), sodium hypophosphite hydrate ($NaH_2PO_2.xH_2O$, Aldrich), and sodium thiosulfate pentahydrate ($Na_2S_2O_3.5H_2O$, ≥99.5%, Aldrich) were used as the sources for Ni, Co, P, and S, respectively. The optimal mixtures of stoichiometric amounts of these precursors were mechanically ground using a mortar and pestle [($NiCl_2.6H_2O$ + $CoCl_2.6H_2O$) = 10 mol%; ($NaH_2PO_2.xH_2O$ + $Na_2S_2O_3.5H_2O$) = 90 mol%)]. The ratio of $NaH_2PO_2.xH_2O$, and $Na_2S_2O_3.5H_2O$ were then correspondingly altered to obtain $(Ni_{0.95}Co_{0.05})_2P$: x at. % S (x= 0, 5, 10, 15) with the desired nominal percentage of S and P in the final system. The resulting solid mixtures were transferred in alumina crucible and the crucibles containing the solid mixtures were subjected to heat treatment in ultra-high purity argon atmosphere (Matheson; 99.99%, flow rate = 100 $cm^3\ min^{-1}$) at 250°C for 1 h (Ramp rate = 10°C min^{-1}). The thermally treated solid mixtures were naturally cooled to room temperature in

continuous Ar gas flow. The obtained products were then crushed using a mortar and pestle and thoroughly washed with ethanol followed by vacuum drying at room temperature.

4. Results and Discussion

4.1 Theoretical study illuminating the effect of Co and S on the electrochemical activity and stability of the $(Ni,Co)_2P$:S compounds

The electrocatalytic activity of any electrocatalyst is anticipated to depend on the electronic structure as well as the electronic conductivity, while the long-term stability of the electrocatalyst is assumed to qualitatively depend on the cohesive energy of the system. The effect of compositions on the electronic and catalytic properties as well as on the structural stability of the material can be investigated from the theoretical studies. As mentioned in the 'Computational Methodology' section, the key purpose of the computational component of the present study is to investigate the effects of Co and S dopants on the electrocatalytic activity as well as the structural and electrochemical stability of Ni_2P during HER. Accordingly, the electronic structure, hydrogen adsorption free energies (ΔG_{H^*}), and the cohesive energies of the materials as a qualitative measure of the electrochemical activity and stability, have all been evaluated for the different electrocatalyst compositions in the present study.

For a good HER electrocatalyst, it is critical that the ΔG_{H^*} should be close to zero which will enable facile adsorption and desorption of hydrogen atoms from the surface of the electrocatalyst during HER. Therefore, it is imperative to estimate the free binding

energy of the hydrogen to the electrocatalytic surface. Accordingly, modification of the electrocatalytic surface electronic structure by altering the chemical composition in such a way that the resulting ΔG_{H^*} is close to zero can significantly improve the electrocatalytic activity of the material. Thus, the hydrogen binding free energies have been obtained from DFT calculations by subtracting the free energy of the pristine electrocatalyst surface and a half of a hydrogen molecule in the gas phase from the corresponding free energy of the electrocatalyst surface with hydrogen atom bonded to the site according to **eq. 1**. Similar methodology has been used in the computational study by Nørskov et al. in the previous report.[19]

Table 1 tabulates the values of the ΔG_{H^*}, density of states at the Fermi level [$N(E_F)$], and cohesive energies (E_{coh}) for all the different materials considered in the present study. It can be seen that the adsorption of hydrogen to the surface of pure Ni_2P is too weak and quite far from the optimal value which results in an inferior electrocatalytic activity for HER. From the electronic structure consideration, it can be inferred that since Ni-3d electrons locate relatively deep below the Fermi level (the Ni-3d band center lies around -2.2 eV vs. Fermi level), the hybridization between these electrons and H-1s states located above the Fermi level becomes very weak and thus, renders the adsorption of hydrogen atoms practically impossible (**Figure 1b**).

It is noteworthy however, that introduction of Co into the Ni_2P lattice; substituting for Ni reduces the ΔG_{H^*} noticeably bringing its value toward the more optimal energy value (**Figure 1c**). Herein, new Co-3d electronic states are generated, locating closer to the Fermi level and hybridize with H-1s electrons slightly better resulting in stronger interaction between hydrogen atoms and the surface of the material (in particular, with Co atoms). This result is also ably supported by the fact that the decomposition energy of diatomic molecule Co-H is ~245 kJ mol^{-1}, while the same for Ni-H molecule is ~240 kJ mol^{-1}, which is slightly weaker.[23] Such alteration in the electronic structure is anticipated to advance the electrocatalytic activity of the electrocatalyst (**Figure 1b**). The substitution of phosphorus by sulfur in $(Ni_{0.83}Co_{0.17})_2P$ brings the hydrogen adsorption energy even more closely to the zero value of ~0.1 eV. This result demonstrates improvement in the strength of the hydrogen-surface interaction due to the stronger H-S bonds in comparison to the H-P bonds (bond dissociation energies for diatomic molecules are 353.6 kJ mol^{-1} *vs*. 297.0 kJ mol^{-1}, respectively).[23] This outcome of the sulfur addition is estimated to further increase the electrocatalytic activity of $(Ni_{0.83}Co_{0.17})_2P$:S. Thus, utilizing the concept of free energy of hydrogen adsorption to the electrocatalytic surface, the present study has demonstrated the beneficial effect of incorporation of Co and S on the expected catalytic activity of Ni_2P electrocatalyst for HER. In addition, both the incorporation of S dopant and the presence of P vacancy can both effectively optimize the ΔG_{H^*}, remarkably promoting the desorption of H* and thus, the HER activity.[24, 25]

Also, by replacing P with S, more electrons are taken from the metal atoms. Therefore, the desorption of the HER intermediates can be promoted by the substitution of P with S, ultimately increasing the utilization rate of the Co active sites. Accordingly, utilizing the concept of ΔG_{H^*}

toward the electrocatalytic surface, the beneficial effect of incorporation of Co and S on the expected HER electrocatalytic activity of Ni_2P is anticipated.

Furthermore, the additional goal of the present study as delineated earlier is to inspect the effect of Co and S doping on the electronic conductivity of Ni_2P. It is well-known that the metallic conductivity is directly proportional to the $N(E_F)$. Thus, the study of density of states indeed offers a qualitative evaluation of the influence of these dopants on the overall electronic conductivity of Ni_2P. The electronic structure of pure Ni_2P as well as the phosphide doped with Co and S calculated in the present study demonstrates a metal-type conductivity for all the three compositions of the proposed electrocatalysts with non-zero density of the electronic states at the Fermi level (**Figure 1b)**. However, the values for the density of electronic states at the Fermi level are different indicating slight improvement in the electronic conductivity with the introduction of Co and S into the Ni_2P crystal structure (see **Table 1**).

The incorporation of Co into the Ni_2P system thus alters the electronic structure to relay the presence of Co-3d electrons in the vicinity of the Fermi level which increases

the number of electrons. This therefore results in a slight improvement in the overall electronic conductivity of the material (**Figure 1b**). Introduction of S into the $(Ni_{0.83}Co_{0.17})_2P$ lattice by substituting for P atoms further improves the conductivity, as the sulfur atoms bind to lower number of Ni- and Co- 4s valence electrons than phosphorus atoms (2 electrons for each S instead of 3 electrons for each P atom). This makes some of Ni- and Co- valence electrons free in the system and thus increases the number of total charge carriers at the Fermi level, as depicted in **Table 1**. Such improvements in the electronic conductivity is beneficial for the overall electrocatalytic activity of the material while also favoring the hydrogen adsorption energy to the surface of the electrocatalyst.

Furthermore, another goal of the present theoretical study is the investigation of structural and electrochemical stability of the HER system. This has been gathered by evaluating the cohesive energy E_{coh}. A higher E_{coh} (more negative value) consequently, suggests a higher stability of the electrocatalyst material. **Table 1** shows the E_{coh} calculated for the various electrocatalyst compositions. It can be seen that an introduction of Co into the Ni_2P lattice noticeably increases the cohesive energy and thus, offers improvement in the overall stability of $(Ni_{0.83}Co_{0.17})_2P$ due to the presence of the stronger Co-P bonds in comparison to Ni-P [calculated E_{coh} for pure Ni_2P is -15.41 eV/formula unit vs. -15.57 eV/formula unit for $(Ni_{0.83}Co_{0.17})_2P$]. Nevertheless, further

introduction of S into the $(Ni_{0.83}Co_{0.17})_2P$ compound results in reducing the cohesive energy which occurs mainly due to the lower ionic charge of S^{2-} *vs.* P^{3-} and thus, leads to significantly weakening of the electrostatic component of Ni-S and Co-S bonds than those of Cu-P and Co-P ionic bonds. Despite a relative decrease in the cohesive energy of $(Ni_{0.83}Co_{0.17})_2P_{0.67}S_{0.33}$, the overall chemical and structural stability of the material is preserved and is not significantly compromised by the introduction of S into the system. The substitution and incorporation of S therefore, makes this material capable of withstanding the harsh electrochemical conditions during HER.

Consequently, on the basis of the present DFT study, $(Ni,Co)_2P$:S is expected to reveal improved electrochemical performance owing to its optimal hydrogen adsorption energy and improved electronic conductivity, along with the good structural and electrochemical stability. Such beneficial modification of the electronic structure provides favorable electrocatalytic attributes to this material making it an excellent candidate for HER electrocatalysis. Accordingly, pre-empted by the DFT study, in order to validate these theoretical results, in the present study, experimental synthesis and characterization of different compositions of $(Ni_{0.95}Co_{0.05})_2P$: x at. % S (x=5, 10, 15) have been conducted, the results of which are elucidated in the following sections.

4.2 Experimental Results

4.2.1 Structural characterizations

The crystalline phase structure and phase purity of as-synthesized electrocatalysts have been characterized by the powder X-ray diffraction (XRD) analysis. The XRD patterns of as-

synthesized Ni_2P (**Figure 3a**) show a hexagonal structure (space group P^{-}_{62m}, JCPDS card no: 74-1385) with lattice parameters a = b = 5.859 Å, c =3.382 Å, and unit cell volume of ~116.096 $Å^3$ **(Table 2**), which is in good agreement with the previously reported literature results. [20, 21] As shown in **Figure 3b**, Co doped Ni_2P i.e. $(Ni_{0.95}Co_{0.05})_2P$ exhibits a hexagonal structure, similar to pure Ni_2P with a slight negative peak shifts toward lower diffraction angles, reflective of the expected lattice expansion upon cobalt (5 at. %) incorporation into the Ni_2P lattice. This result has been further substantiated by increase in the lattice parameters and unit cell volume of $(Ni_{0.95}Co_{0.05})_2P$ (**Table 2**). As also seen from **Figure 3c, d, and e**, all the XRD powder diffraction pattern reflections of $(Ni_{0.95}Co_{0.05})_2P$:S with different S concentrations show XRD peaks corresponding to single phase hexagonal structured $(Ni_{0.95}Co_{0.05})_2P$, devoid of any other peaks corresponding to any undesired secondary phases of S-based compounds. In addition, increasing S concentrations in the $(Ni_{0.95}Co_{0.05})_2P$ results in gradual shifts toward lower diffraction angles for the XRD peaks, which further affirms to the successful incorporation of S into the $(Ni_{0.95}Co_{0.05})_2P$ lattice. Similar results depicting slight negative shifts in peak positions are witnessed and documented in earlier published reports of S-doped $CoSe_2$ electrocatalyst.[26] Furthermore, as tabulated in **Table 2,** the lattice parameters and unit cell volume of S containing electrocatalysts exhibit slight increase with increasing S concentrations, demonstrating slight lattice expansion upon S incorporation which is also in good agreement with the various S doped electrocatalysts reports in the literature.[3] Therefore, these XRD results suggest the successful S incorporation and formation of single phase solid solutions of $(Ni_{0.95}Co_{0.05})_2P$: S in the synthesized electrocatalysts. It is also important to mention here that at higher S concentration i.e. $(Ni_{0.95}Co_{0.05})_2P$: 20S, the destruction of advantageous solid solution (**Figure S1**) is witnessed, with a consequent phase separation into NiS, NiS_2, CoS_2, and Ni_2P. It is moreover, well known that typically mixed phase

of electrocatalyst systems demonstrate lower electrochemical performance in comparison to the single phase solid solution systems.[27, 28] In a recent review article detailin the stability challenges for OER-HER electrocatalysts, Strasser and co-workers[27] elucidated that the formation of a solid solution or single-phase electrocatalyst is often a critical prerequisite for achieving good performance of multi-metallic electrocatalysts. On the other hand, the different activity and conductivity of the materials in the mixed (multi-phase) electrocatalysts will preferably corrode the less stable material, consequently, leading to increased deterioration in electrochemical activity and stability, which is indeed observed for the electrochemical performance of higher sulfur containing $(Ni_{0.95}Co_{0.05})_2P$: 20S electrocatalysts.

The morphology and quantitative elemental compositions of the representative $(Ni_{0.95}Co_{0.05})_2P$: 15S electrocatalyst have been characterized by SEM-EDX measurements. **Figure 4a** shows the SEM image of as-synthesized $(Ni_{0.95}Co_{0.05})_2P$: 15S electrocatalyst. The EDX pattern of $(Ni_{0.95}Co_{0.05})_2P$: 15S (**Figure 4b**) shows the co-existence of Ni, Co, P, and S elements. Quantitative elemental composition analysis of $(Ni_{0.95}Co_{0.05})_2P$: 15S obtained from EDX shows the measured elemental composition (i.e. Ni, Co, P, and S as 63.20, 3.37, 28.16, and 5.27 at. %, respectively) in good agreement with the desired experimental composition, with P:S ratio obtained as ~ 0.8423:0.1577 which is very close to the expected ratio of 85:15. Furthermore, the elemental mapping results of Ni, Co, S, and P of $(Ni_{0.95}Co_{0.05})_2P$: 15S **(Figure 4c, d)** reveal the uniform distribution of elements within the as-synthesized particles of $(Ni_{0.95}Co_{0.05})_2P$: 15S electrocatalyst powder, devoid of any impurities or segregation at any specific site.

The static water contact angle method was employed to investigate the wetting characteristics of the as-synthesized electrocatalysts. As shown in **Figure 5**, pure Ni_2P demonstrates a good

wettability (hydrophilic nature) with an average water contact angle of ~42°. Next, $(Ni_{0.95}Co_{0.05})_2P$, $(Ni_{0.95}Co_{0.05})_2P$: 5S, $(Ni_{0.95}Co_{0.05})_2P$: 10S, and $(Ni_{0.95}Co_{0.05})_2P$: 15S electrocatalysts were tested all of which exhibit water contact angles of ~35°, ~17°, ~12°, and ~7°, respectively, indicating progressive enhancement in wettability of the Co and S doped electrocatalysts in comparison to that of pristine Ni_2P. These results thus suggest the improved affinity of the multi-element containing heterogeneous electrocatalysts for the hydrogen evolution reaction, which in turn can lead to enhancement in their electrocatalytic activities for acid mediated HER.[29] In this regard, various researchers report that the formation of polar bonds by elemental doping as well as by increasing dopant concentrations in the parent electrocatalyst can enhance the wetting characteristic of the doped electrocatalyst. [29, 30] Furthermore, in order to gain deeper insights into the contact angle analysis, employing the Fritz correlation, bubble break-off (or departure) diameters for the as-synthesized electrocatalysts were calculated.

The expression of the Fritz correlation[31] is written as: $D_{dp} = 0.20 \times \theta \times \left(\frac{\sigma}{g(\rho_l - \rho_g)}\right)^{0.5}$, where D_{dp} refers to the bubble break-off diameter (m), θ is the contact angle (degree), σ refers to liquid–air surface tension (N m^{-1}), g refers to the acceleration due to gravity (m^2 s^{-1}) and, ρ_l and ρ_g are the density of liquid (water) and gas (air) in units of kg m^{-3}, respectively. According to this equation, a lower contact angle value leads to smaller H_2 bubble diameters. The calculated bubble break-off diameter values for the as-synthesized electrocatalysts are shown in **Figure 5**. As can be gleaned from these results, $(Ni_{0.95}Co_{0.05})_2P$: 15S electrocatalyst demonstrates the smallest bubble break-off diameter (~0.38 mm) in comparison to the other synthesized compositions and thus, suggests an expected faster separation of H_2 from the electrode surface. Such characteristics are

not only beneficial to free the active sites for subsequent hydrogen evolution reactions, but also to decrease the ohmic resistance (R_Ω) of the electrode, ultimately offering improvement in electrocatalytic activity and HER performance.[32] Accordingly, smaller contact angle and bubble break-off diameter of $(Ni_{0.95}Co_{0.05})_2P$:15S electrocatalyst composition ensures the facile electrolyte penetration as well as rapid H_2 separation from electrode surface, thus leading to expected improved HER kinetics.

X-ray photoelectron spectroscopy (XPS) analysis was also performed to investigate the chemical valence states of Ni, P, Co, and S of the as-synthesized pure Ni_2P and the substituted $(Ni_{0.95}Co_{0.05})_2P$: 15S. As depicted in **Figure 6a** , the XPS spectrum in the Ni $2p_{3/2}$ region for pure Ni_2P shows a peak ~ 852.7 eV which is in good agreement with the earlier published reports.[33] The XPS spectrum of P 2p (for Ni_2P) (**Figure 6b**) shows two peaks at ~129.4 and ~133.91 eV which can be ascribed to P $2p_{3/2}$ in Ni_2P and phosphate species (PO_4^{3-}), respectively which can be formed due to the partial oxidation of the surface upon exposure of the Ni_2P particles to air which is commonly observed in all of the various phosphide based electrocatalyst materials reported in the literature.[3] Furthermore, it is important to highlight that the peak at ~ 852.7 eV in the Ni $2p_{3/2}$ region of pure Ni_2P (**Figure 6a**) exhibits higher binding energy in comparison to the metallic Ni (~ 852.6 eV)[34] whereas the dominant peak at ~129.4 eV in the P 2p region of pure Ni_2P (**Figure 6b**) reflects a lower binding energy in comparison to the elemental P (~130.2 eV).[35] These results indicate that the Ni metal centers possess a positive partial charge (δ^+) and P pendant bases contain negative partial charge (δ^-), suggesting the transfer of electrons from Ni to P and thus, modification of the charge density of Ni and P in Ni_2P. [3, 36] The obtained results are also indeed in good agreement with various doped (Co, Fe) phosphide electrocatalysts (Co-Cu_3P, Fe-Ni_2P).[3]

In the case of the substituted and doped phosphosulfide, it is important to note that the Ni $2p_{3/2}$ peak for $(Ni_{0.95}Co_{0.05})_2P$:15S (**Figure 6a**) demonstrates a higher binding energy value with a positive shift of ~ 0.35 eV in comparison to pristine Ni_2P. This positive shift in the XPS binding energy implies the transfer of electrons from Ni to S and correspondingly, a modification of the charge density due to the formation of the solid solution of phosphosulfide.[37] Similar result of positive shift in the binding energy is observed for the P $2p_{3/2}$ peak of $(Ni_{0.95}Co_{0.05})_2P$:15S which again interprets the modification of electronic structure (as is also substantiated by the DFT results) of the doped and substituted electrocatalyst.

Additionally, in the XPS spectrum of Co 2p (**Figure 6c**), the peak at ~779.42 eV can be accredited to Co $2p_{3/2}$ in $(Ni_{0.95}Co_{0.05})_2P$: 15S (which corresponds to Co species in CoP). It is observed that this peak at ~ 779.42 eV contains a shift of ~0.22 eV to higher binding energy in comparison to the typical peak (at ~779.2 eV) in the Co $2p_{3/2}$ region of CoP[38], which can be attributed to electron transfer from Co to S. Moreover, it should be noted that the Co $2p_{3/2}$ peak possesses a higher binding energy than that of metallic Co (~778.4 eV). As elucidated above, this result also suggests the existence of Co (metal centers) with a partial positive charge (δ^+) and P and S (pendant bases) with partial negative charge (δ^-) close to metal center, and consequently, indicating the transfer of electrons from Co to P and S as well as the beneficial improvement in the electronic structure of the $(Ni_{0.95}Co_{0.05})_2P$: 15S electrocatalyst due to the substitution and incorporation of S and Co into the Ni_2P lattice structure.[3]

Next, as depicted in the **Figure 6d**, the XPS spectrum of $(Ni_{0.95}Co_{0.05})_2P$:15S in the S 2p region displays a major peak at ~161.16 eV corresponding to the S $2p_{3/2}$ which is in accordance

with the S containing phosphide electrocatalysts.[3] Furthermore, to shed more light on the as-obtained XPS results, in the various literature studies it has been reported that the proton relays which are incorporated in a metal complex HER electrocatalyst arise from the pendant acid-base groups. Such groups are adjacent to the metal centers wherein HER is known to occur.[36, 39, 40] The active sites for metal complex hydrogenase enzyme also possess pendant bases which are close to the metal centers.[36, 41] Accordingly, as described above in the XPS results, the as-obtained $(Ni_{0.95}Co_{0.05})_2P$:15S exhibits metal centers Ni, Co (δ^+) and pendant bases P, S (δ^-) that are situated close to the metal centers.[3, 36] It is therefore expected that $(Ni_{0.95}Co_{0.05})_2P$:15S will likely unveil hydrogen evolution mechanism analogous to those of metal complex hydrogenase enzymes reported in the literature.[3, 36] Based on the above analyses, Ni, Co, P, and S in the active $(Ni_{0.95}Co_{0.05})_2P$:15S electrocatalyst can thus likely exhibit hydride-acceptor and proton-acceptor centers, respectively.[3, 36] Based on the above combination of promising attributes, it can be speculated that the Co and S containing Ni_2P solid solution can offer superior electrochemical response for the hydrogen evolution reaction as documented and described in the sections to follow.

4.2.2 Electrochemical characterization of electrocatalysts

The HER activity of as-synthesized electrocatalysts was evaluated in 1N H_2SO_4 solution using a typical three-electrode cell comprising platinum wire as the counter electrode as described in the **Supplementary Information**. **Figure 7a** shows the HER polarization curves of the as-prepared electrodes. The electrochemical performance of the electrodes was compared with state-of-the art commercial Pt/C as a benchmark HER electrocatalyst. As shown in **Figure 7a**, the current collector - Ti substrate expectedly demonstrates negligible current density in comparison

to all of the other active electrocatalysts synthesized and used in the current study and thus, suggests its poor electrochemical activity towards the acid mediated HER. In sharp contrast, the as-synthesized Ni_2P exhibits good HER response by exhibiting an over-potential of 112 mV and 450 mV to deliver current density of 10 and 100 mA cm^{-2}_{geo}, respectively (**Table 2**). Also, in good agreement with the DFT results, the Co doped Ni_2P [$(Ni_{0.95}Co_{0.05})_2P$] demonstrates significantly improved HER activity by attaining a current density of 10 mA cm^{-2}_{geo} at an over-potential of 74 mV, 38 mV lower than that of Ni_2P. This activity improvement is attributed to enhanced reaction kinetics (lower activation polarization), reduced hydrogen adsorption free energy, and lower charge transfer resistance (R_{ct}) than Ni_2P as evidently confirmed by the electrochemical impedance spectroscopy (EIS) analysis, discussed later. It is important to highlight that this obtained result is in excellent agreement with the previous literature reports wherein Co incorporation significantly improved the HER kinetics.[3]

These studies conclude that the introduction of Co into the parent electrocatalyst material optimizes the overall electronic structure of electrocatalyst, offering reduction of the kinetic energy barrier of H atom adsorption (ΔG_{H^*}) for the doped electrocatalyst and thus, gives rise to improved reaction kinetics and electrocatalytic activity. Furthermore, it is interesting to note that S incorporation into the $(Ni_{0.95}Co_{0.05})_2P$ system noticeably enhances the HER activity. It can be seen from **Figure 7a and Table 2** that $(Ni_{0.95}Co_{0.05})_2P$:15S composition demonstrates higher activity by delivering a current density of 10 mA cm^{-2}_{geo} at an over-potential of only 44 mV whereas Pt/C, $(Ni_{0.95}Co_{0.05})_2P$:10S, $(Ni_{0.95}Co_{0.05})_2P$:5S, and $(Ni_{0.95}Co_{0.05})_2P$ display overpotentials of ~ 42, 52, 63, and 74 mV, respectively. These results thus clearly suggest that the HER kinetics and activity of $(Ni_{0.95}Co_{0.05})_2P$:15S is comparable to Pt/C and much superior to other PGM-free as-synthesized

electrocatalysts. Such enhanced HER activity upon incorporation of optimal amount of S can be ascribed to the further improvement in the electronic structure, charge transfer, and reduction in ΔG_{H^*}, as evidently demonstrated by the DFT results. It is also important to mention here that the $(Ni_{0.95}Co_{0.05})_2P$:20S composition exhibits significantly lower HER activity (**Figure S2**) in comparison to other studied compositions. As elucidated in the XRD discussions, such reduction in the electrocatalytic activity can be attributed to destruction of the advantageous solid solution state of the electrocatalyst (**Figure S1**). Similarly, in the literature, various electrocatalysts with different degree of S concentration are reported for HER as well as OER wherein after a certain concentration of S doping, there is decline in the electrocatalytic activity.[42, 43] According to these reports, the excess S concentration hinders the contact between the active sites on the electrocatalyst and reactant (i.e. blocking the active sites), which correspondingly causes a reduction in the electrochemical activity thus displaying a relatively lower HER activity than the sample with appropriate proportion of S. Thus, in the present system, 15 at. % S is observed as an optimal S concentration that exhibits no phase separation, and shows superior HER activity in comparison to 5, 10, and 20 at. % S compositions.

Furthermore, in order to evaluate the interfacial/charge transfer kinetics of hydrogen evolution reaction, electrochemical impedance spectroscopy (EIS) analysis was conducted at -0.05 V *vs* RHE in the frequency range of 100 mHz-100 kHz with an amplitude of 10 mV, using the circuit model of $R_\Omega(R_{ct}Q_1)$. As depicted in **Figure 7b,** the EIS plot of the as-prepared electrodes show a well-formed semicircular arc wherein the diameter of semicircular arc represents the surface charge transfer resistance (R_{ct}) while the initial point of semi-circular arc on the X-axis represents the ohmic resistance (R_Ω). It can be seen from **Figure 7b** that the pristine Ni_2P exhibits higher ohmic ($R_\Omega \sim 17.05\ \Omega\ cm^2$) as well as higher surface charge transfer resistance ($R_{ct} \sim 25\Omega$

cm^2) (**Table 2**). The R_Ω as well as R_{ct} values for $(Ni_{0.95}Co_{0.05})_2P$ on the other hand, are obtained as ~ 16.6 Ω cm^2 and ~ 19 Ω cm^2, respectively. The reduction in the resistance values suggest the improved charge transfer kinetics in comparison to that of Ni_2P. In addition, the S-doped electrocatalysts demonstrate further reduction in the impedance values, with a lowest values of R_Ω ~ 15 Ω cm^2 and R_{ct} ~ 6.82 Ω cm^2 obtained for $(Ni_{0.95}Co_{0.05})_2P$:15S in comparison to all of the other electrocatalysts containing 10S and 5S compositions. Moreover, the R_Ω and R_{ct} values of the $(Ni_{0.95}Co_{0.05})_2P$:15S electrocatalyst are almost similar to commercial Pt/C (**Table 2**). Consequently, these results evidently reflect the higher charge transfer rate and faster HER kinetics achieved for the optimum composition of $(Ni_{0.95}Co_{0.05})_2P$:15S. It is also important to mention that, since pure Ni_2P and $(Ni_{0.95}Co_{0.05})_2P$:15S exhibit comparable surface area (~1.55 m^2g^{-1}), the enhanced charge transfer kinetics and HER activity is attributed to the optimized surface electronic structure of Co and S containing $(Ni_{0.95}Co_{0.05})_2P$:15S for HER as well as lower water contact angle ensuring the facile electrolyte penetration and thus, offering lower ohmic as well as charge transfer resistance. The mass activity and turn over frequency for the $(Ni_{0.95}Co_{0.05})_2P$:15S electrocatalyst is also superior compared to the other electrocatalysts studied in this work (**Table S1**).

Additionally, in order to obtain more insights into the electrochemical kinetics of as-synthesized electrocatalysts and compare their HER activity, as depicted in **Figure 7c**, Tafel slopes and over-potential to attain the current density of 50 mA $cm^{-2}{}_{geo}$ are reported. As shown in **Figure 7c**, $(Ni_{0.95}Co_{0.05})_2P$:15S demonstrated smaller Tafel slope (31.25 mV dec^{-1}) and overpotential (85 mV at 50 mA $cm^{-2}{}_{geo}$) which is comparable to that of Pt/C, and is also consistent with the previous literature of Pt/C while also being remarkably lower than all of the other as-synthesized electrocatalyst (**Figure S4, Table S2**).[3] Typically, three possible reaction steps are known for the HER in acidic electrolytes namely, the discharge step (Volmer reaction, $H_3O^+ + e^- \rightarrow H_{ads} + H_2O$),

the catalytic recombination step (Tafel reaction, $H_{ads} + H_{ads} \rightarrow H_2$), and finally, the electrochemical desorption step (Heyrovsky reaction, $H_{ads} + H_3O^+ + e^- \rightarrow H_2 + H_2O$). In this context, the comparable Tafel slope values achieved for $(Ni_{0.95}Co_{0.05})_2P$:15S and Pt/C suggest that the HER process is dominated by a Volmer-Tafel reaction mechanism, in which the recombination of the two adsorbed species (H_{ads}) is the rate-limiting step.[26] It is important to also note that the Tafel slopes values for the other electrocatalyst compositions are obtained in the range of 40-120 mV dec^{-1}, which implies that the HER would likely occur via a Volmer-Heyrovsky reaction process , wherein electrochemical desorption of H_2 is considered as the rate-limiting step.[26] The HER performance of $(Ni_{0.95}Co_{0.05})_2P$:15S is also superior compared to other reported non-noble metals based electrocatalysts in acid medium (**Table S2)**.

The electrochemical stability of $(Ni_{0.95}Co_{0.05})_2P$:15S was investigated by performing the chronoamperometry (CA) test at constant potential of -0.05 V *vs* RHE. As displayed in **Figure 7d**, the as-synthesized $(Ni_{0.95}Co_{0.05})_2P$:15S demonstrates good HER durability, comparable to that of the state-of-the-art Pt/C, with a negligible change in current density. In addition, as illustrated in **Figure S5**, the response of the $(Ni_{0.95}Co_{0.05})_2P$:15S electrocatalyst following the stability tests, demonstrated no significant change in the activity and charge transfer resistance after the durability test, suggesting robust HER electrocatalysis of the $(Ni_{0.95}Co_{0.05})_2P$:15S in acidic electrolyte. For example, the LSV and EIS of $(Ni_{0.95}Co_{0.05})_2P$:15S following the stability tests reveal negligible change in the electrocatalytic activity (**Figure S5b**) i.e. attaining current density of 10 and 100 mA cm^{-2}_{geo} at an overpotential of only ~ 46 mV and ~108 mV, respectively, and exhibiting R_{ct} and R_Ω of ~ 7.35 and ~ 15.20 Ω cm^2 (at -0.05V), respectively, which are very close to the values exhibited by the $(Ni_{0.95}Co_{0.05})_2P$:15S electrocatalyst electrode prior to the stability test with negligible change. Furthermore, as shown by the post-stability XRD (**Figure S6**), SEM, elemental

map, and EDX results collected on the electrode following the chronoamperometry stability tests (**Figure S7**), the crystal structure, morphology, microstructure, and chemical composition of the electrocatalyst, $(Ni_{0.95}Co_{0.05})_2P$:15S are well-preserved after the stability test operation, indicating the structural robustness and mechanical integrity of the electrocatalyst composition for acidic HER. Furthermore, the post-stability XPS (**Figure S8**) collected on the electrocatalyst following the stability test results clearly reveal no major changes in the oxidation states or peak positions, suggesting the good structural and electrochemical durability of the $(Ni_{0.95}Co_{0.05})_2P$:15S electrocatalyst composition toward acidic HER. Finally, inductively coupled plasma optical emission spectroscopy (ICP-OES) analysis was conducted on the electrolyte solution collected after the CA test for $(Ni_{0.95}Co_{0.05})_2P$:15S of three samples from three independent tests which indicates minimal elemental dissolution in the electrolyte solution (**Table S3**). Consequently, these results suggest the excellent electrochemical stability of $(Ni_{0.95}Co_{0.05})_2P$:15S electrode under the operating conditions of acidic HER.

As described above, the present theoretical and experimental study demonstrate the promising electrochemical performance of $(Ni_{0.95}Co_{0.05})_2P$:15S, comparable to that of commercial Pt/C for acid mediated HER. The as-performed DFT and experimental results elucidate the novel and unique modification of the electronic structure due to the introduction of Co and S in the Ni_2P lattice. Thus, in sum total based on the results discussed above, PGM-free $(Ni_{0.95}Co_{0.05})_2P$:15S electrocatalyst, owing to its facile synthesis, low cost, high wettability, and high electrocatalytic performance is indeed a promising HER electrocatalyst.

5. Conclusions

In summary, utilizing earth abundant materials and implementing a simple solid-state synthesis approach, we have synthesized $(Ni_{0.95}Co_{0.05})_2P$:x at. % S (x =0, 5, 10, 15) and demonstrated the highly active and robust nature of these electrocatalysts for acid mediated HER. The as-synthesized $(Ni_{0.95}Co_{0.05})_2P$:15S possessing optimized hydrogen adsorption free energy (ΔG_{H^*}) and beneficial surface electronic modification from DFT analysis experimentally demonstrated excellent electrocatalytic activity in comparison to that of pure Ni_2P and $(Ni_{0.95}Co_{0.05})_2P$: x at. % S (x = 0, 5, and 10). The $(Ni_{0.95}Co_{0.05})_2P$:15S electrocatalyst exhibited a lower charge transfer resistance (6.82 Ω cm^2), a lower over-potential (44 mV) at 10 $mAcm^{-2}$, a much smaller Tafel slope (31.25 mV dec^{-1}), and a higher mass activity (43.75 A g^{-1}) in comparison to the other electrocatalyst compositions. Additionally, the highly active $(Ni_{0.95}Co_{0.05})_2P$:15S electrocatalyst displayed good long term electrochemical HER stability in the acidic media, with no major degradation in the current density thus, suggesting its excellent structural robustness and mechanical integrity for prolonged HER. The superior electrochemical performance of $(Ni_{0.95}Co_{0.05})_2P$:15S is also adequately supported by our DFT calculations which revealed that the $(Ni_{0.95}Co_{0.05})_2P$:15S composition exhibits the highest electronic density of states at the Fermi level $N(E_F)$ and reduced reaction barrier (0.12 eV) thus, offering improved electrocatalytic activity for HER. Therefore, on the basis of the theoretical calculations and electrochemical studies, the present work demonstrates the excellent promise of simultaneous incorporation of Co and S into Ni_2P to enhance the electrochemical performance of these Co and S containing phosphide systems validating their potential use as electrocatalysts for the highly efficient acid mediated hydrogen evolution reaction.

Conflicts of interest

There are no conflicts to declare.

Author contributions

The original concept of the present work is conceived by S. D. G. S. D. G. performed the synthesis, structural, and electrochemical characterization and analyzed the results of structural and electrochemical characterization of electrocatalyst materials. Theoretical study is conducted by O. I. V. P. M. S. and S.D.G. performed and analyzed XPS results. M. K. D., O. I. V., and P. N. K. made important suggestions to the manuscript components. The current project was supervised by P. N. K.

Acknowledgements

The authors acknowledge the financial support of the National Science Foundation, CBET-Grant 0933141 and CBET-Grant 1511390 for the present research. The authors also acknowledge U.S. Department of Energy, Office of Basic Energy Sciences, Division of Materials Sciences and Engineering, Center for Complex Engineered Multifunctional Materials (CCEMM), and Edward R. Weidlein Chair Professorship funds for offering the electrochemical equipment and facilities for conducting research work. Also, the authors thank the Extreme Science and Engineering Discovery Environment (XSEDE)[44] supported by National Science Foundation grant number ACI-1053575, for offering the computational resources needed to complete the theoretical studies.

Table 1: Calculated free energy of hydrogen adsorption (ΔG_{H^*}), the electronic density of states at the Fermi level [($N(E_F)$], and cohesive energy ($-E_{coh}$) for all materials considered in the present DFT study.

Materials	**ΔG_{H^*} (in eV)**	**$N(E_F)$ el./eV/unit cell**	**$-E_{coh}$ (eV/f. un.)**
Ni_2P	0.25	4.18	15.41
$(Co_{0.17}Ni_{0.83})_2P$	0.21	5.68	15.57
$(Co_{0.17}Ni_{0.83})_2P_{0.67}S_{0.33}$	0.12	6.54	15.35

Table 2: Results of electrochemical characterization for HER of as-synthesized electrocatalysts, performed in 1N H_2SO_4 electrolyte solution at 40°C.

Electrocatalyst Composition	**Lattice parameters (Å)**	**Unit Cell Volume (Å^3)**	**R_Ω (Ω cm^2)**	**R_{ct} (Ω cm^2)**	**Overpotential at 10 mA cm^{-2} $_{geo}$ (mV)**	**Overpotential at 100 mA cm^{-2} $_{geo}$ (mV)**	**Tafel slope (mV dec^{-1})**	**Mass Activity (A g^{-1})**
Ni_2P	a = b = 5.859, c =3.382	116.09	17.05	25	112	450	121.3	6.85
$(Ni_{0.95}Co_{0.05})_2P$	a = b = 5.871, c =3.396	117.05	16.6	19	74	385	75.92	12.67
$(Ni_{0.95}Co_{0.05})_2P$:5S	a = b = 5.872, c =3.398	117.16	16.35	14	63	308	73.64	20.55
$(Ni_{0.95}Co_{0.05})_2P$:10S	a = b =5.874, c =3.399	117.27	15.62	9	52	197	52.31	30.45
$(Ni_{0.95}Co_{0.05})_2P$:15S	a = b =5.875, c =3.402	117.42	15	6.82	44	102	31.25	43.75
Pt/C	---	---	14.95	6.25	42	95	30	45

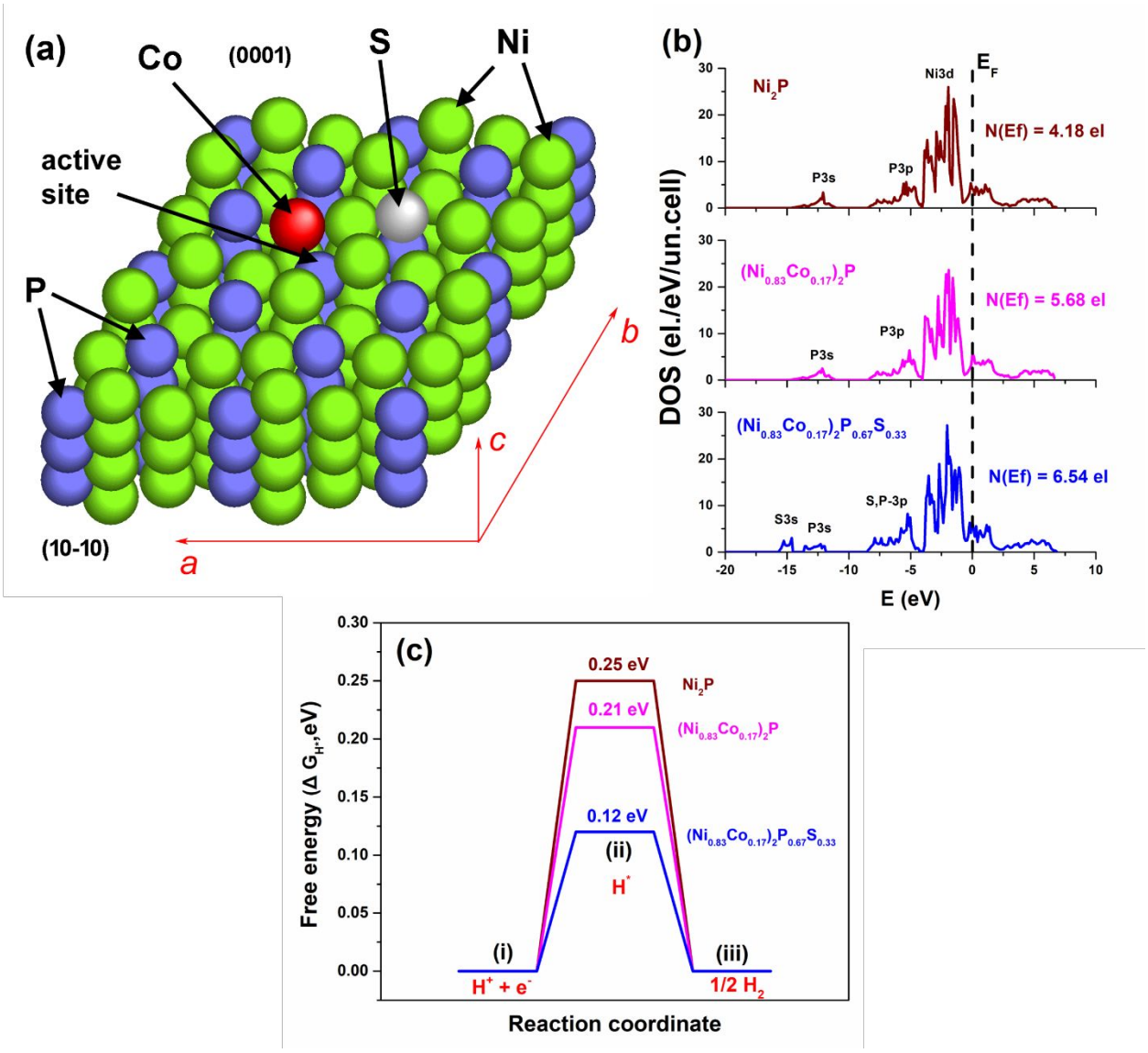

Figure 1. (a) Crystal structure of Ni_2P with Ni_3P_2 termination of (0001) surface. Green atoms – Ni, blue - P, gray - S, and red - Co. Arrow denotes triple-Ni active sites. Vectors ***a***, ***b***, and ***c*** correspond to the bulk crystal structure lattice parameter directions, (b)

calculated total density of electronic states for pure Ni_2P, $(Ni_{0.87}Co_{0.17})_2P$, and $(Ni_{0.87}Co_{0.17})_2P_{0.67}S_{0.33}$; Fermi level is set to zero energy. Labels indicate major contributions from corresponding projected electronic states, and (c) free energy with respect to HER reaction pathway.

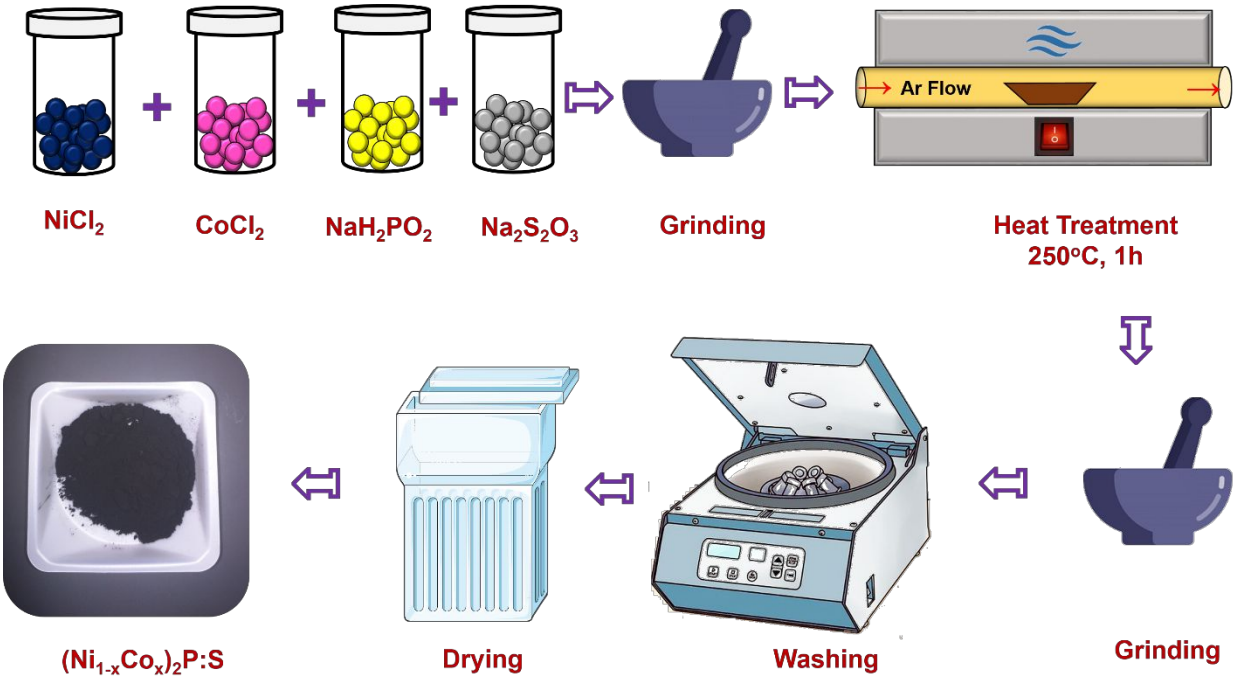

Figure 2. Schematic illustration for the synthesis process of $(Ni_{0.95}Co_{0.05})_2P$:x at. % S electrocatalysts.

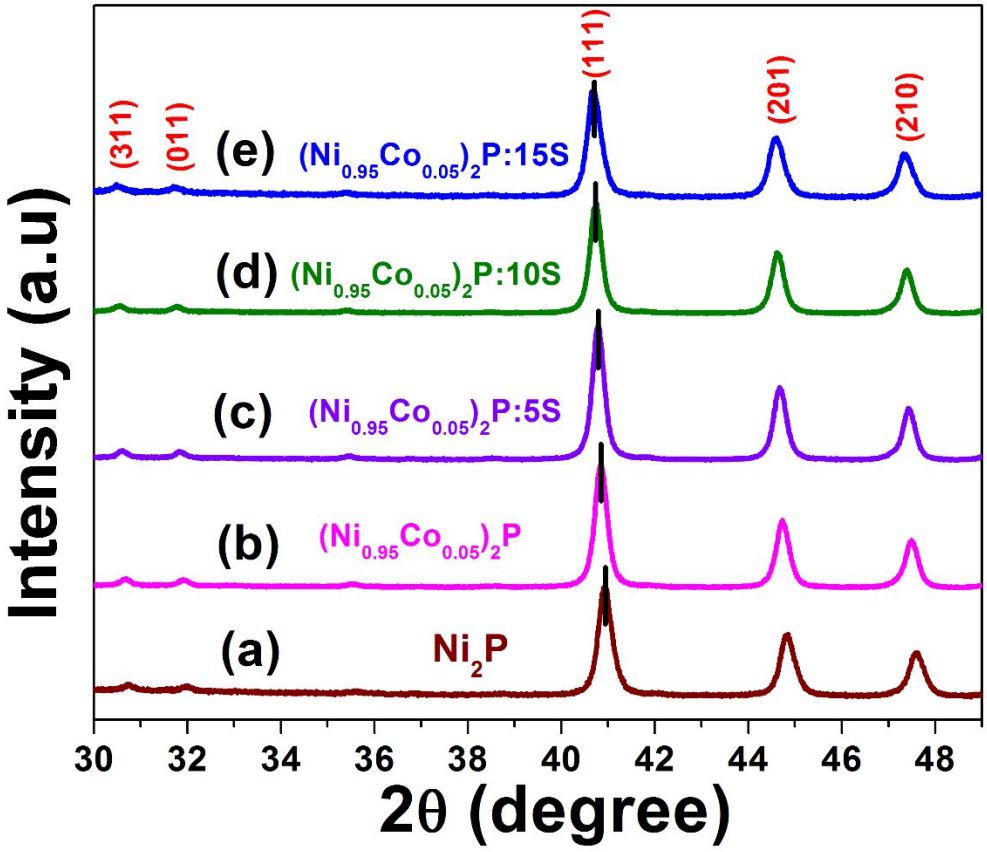

Figure 3. Powder XRD patterns of as-synthesized electrocatalysts.

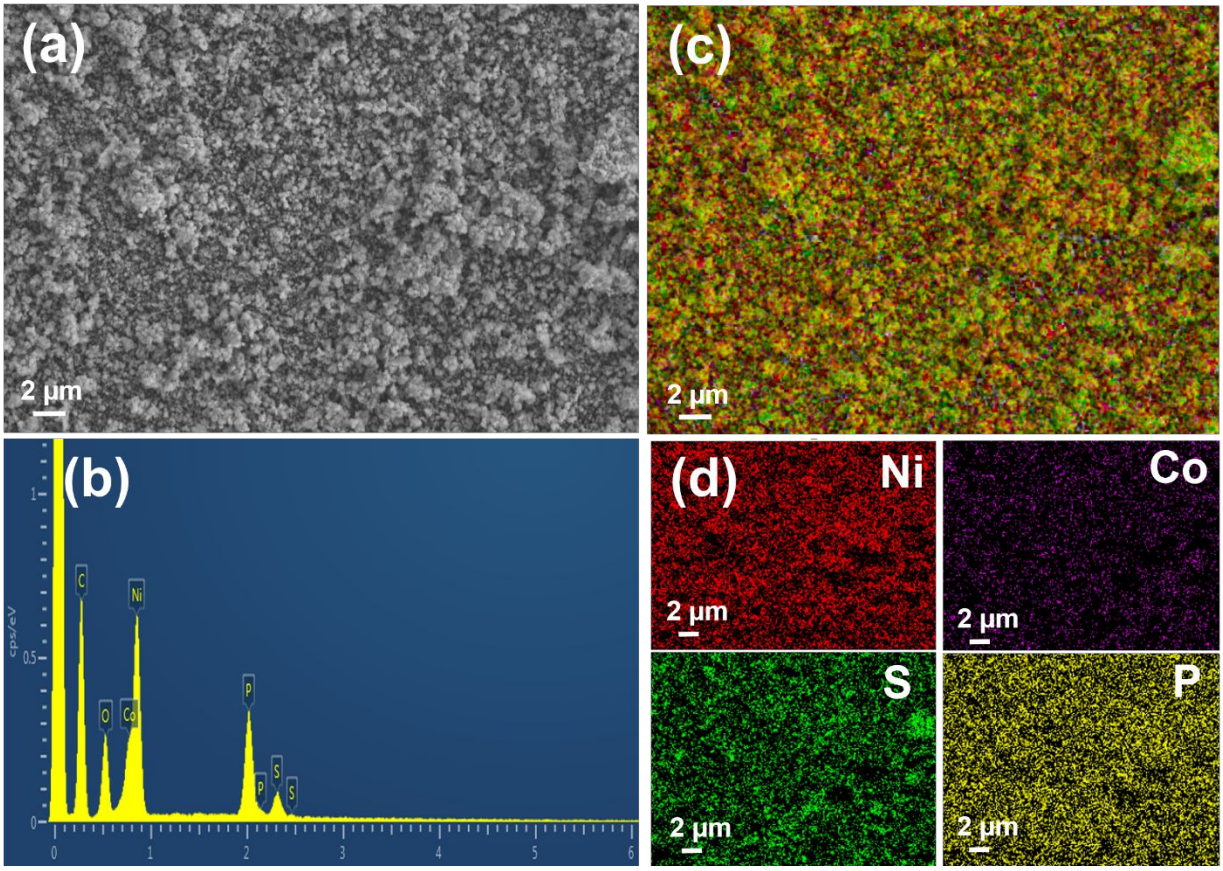

Figure 4. (a) SEM micrograph, (b) EDX spectrum, and (c, e) elemental x-ray mappings for $(Ni_{0.95}Co_{0.05})_2P$: 15S.

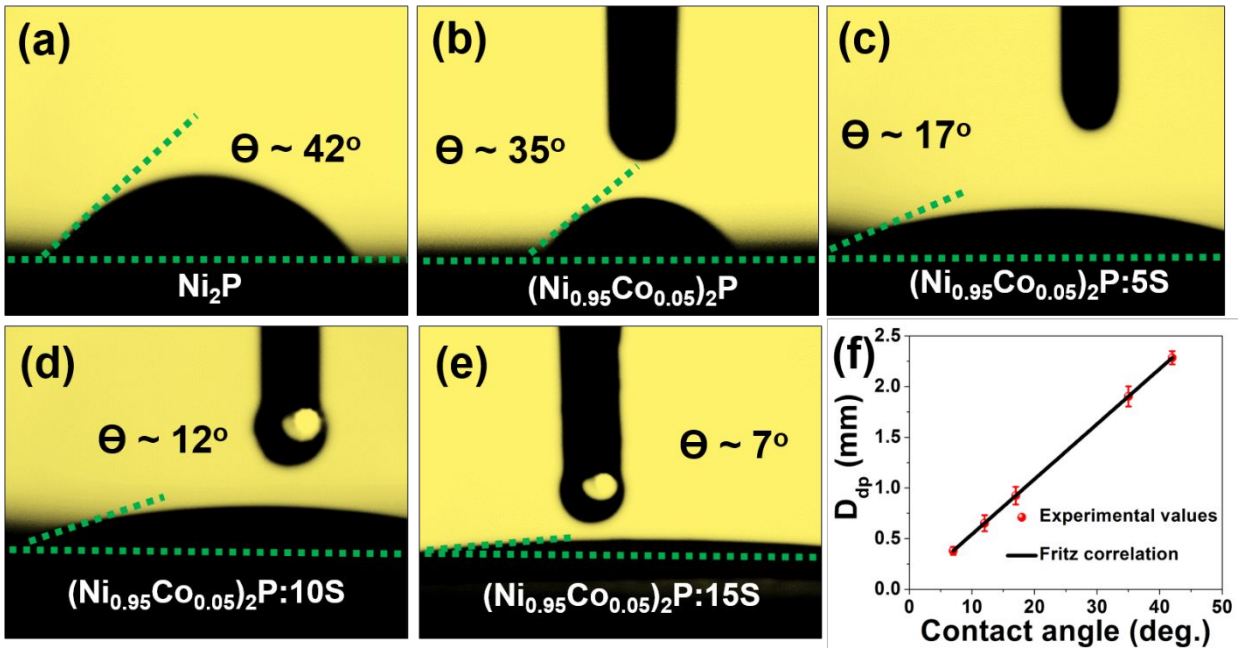

Figure 5. (a-e) Contact angles, and (f) bubble break-off diameters for as-synthesized electrocatalysts.

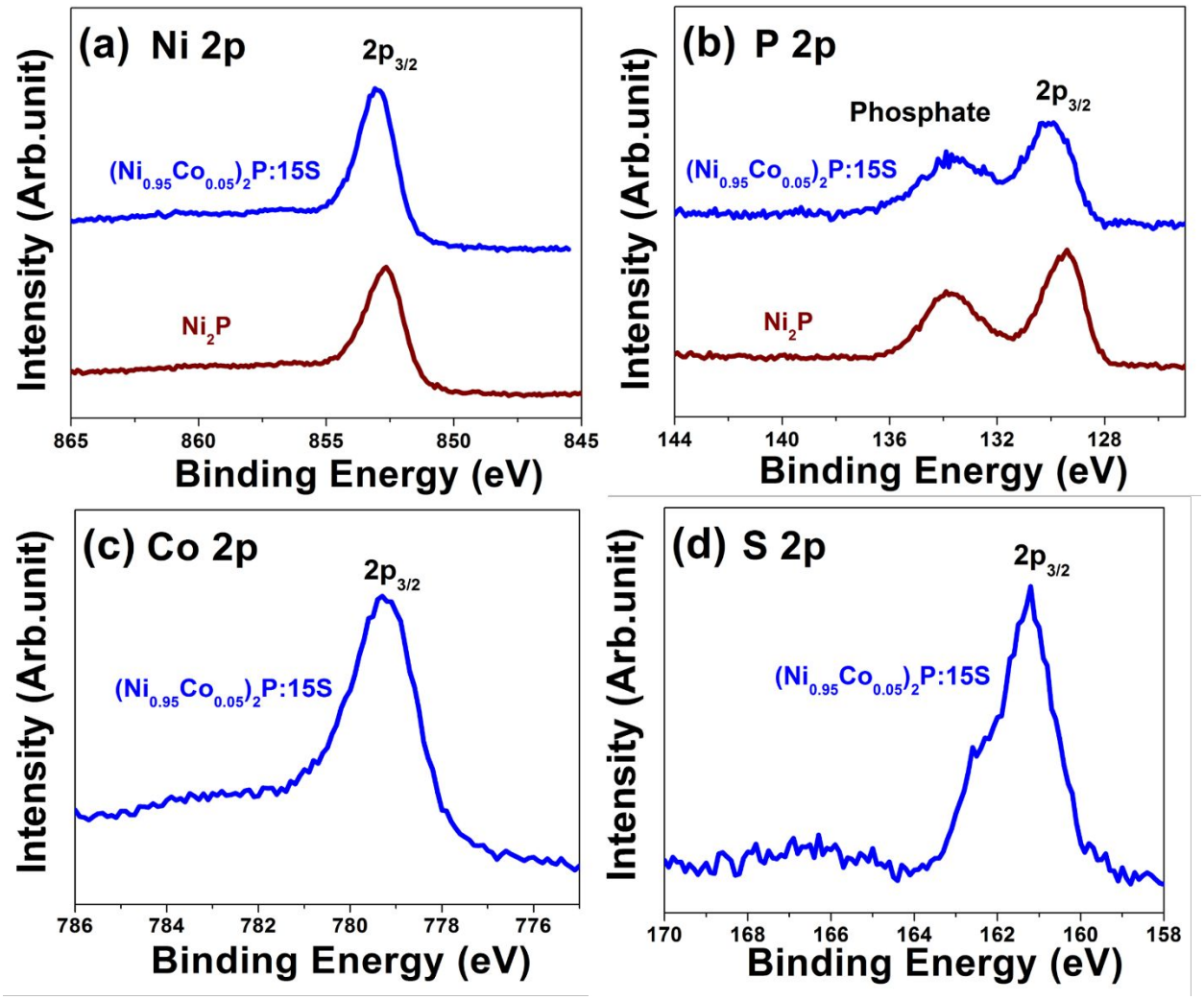

Figure 6. (a) XPS spectra for (a) Ni 2p, (b) P 2p, (c) Co 2p, and (d) S 2p of the $(Ni_{0.95}Co_{0.05})_2P$: 15S and Ni_2P electrocatalysts.

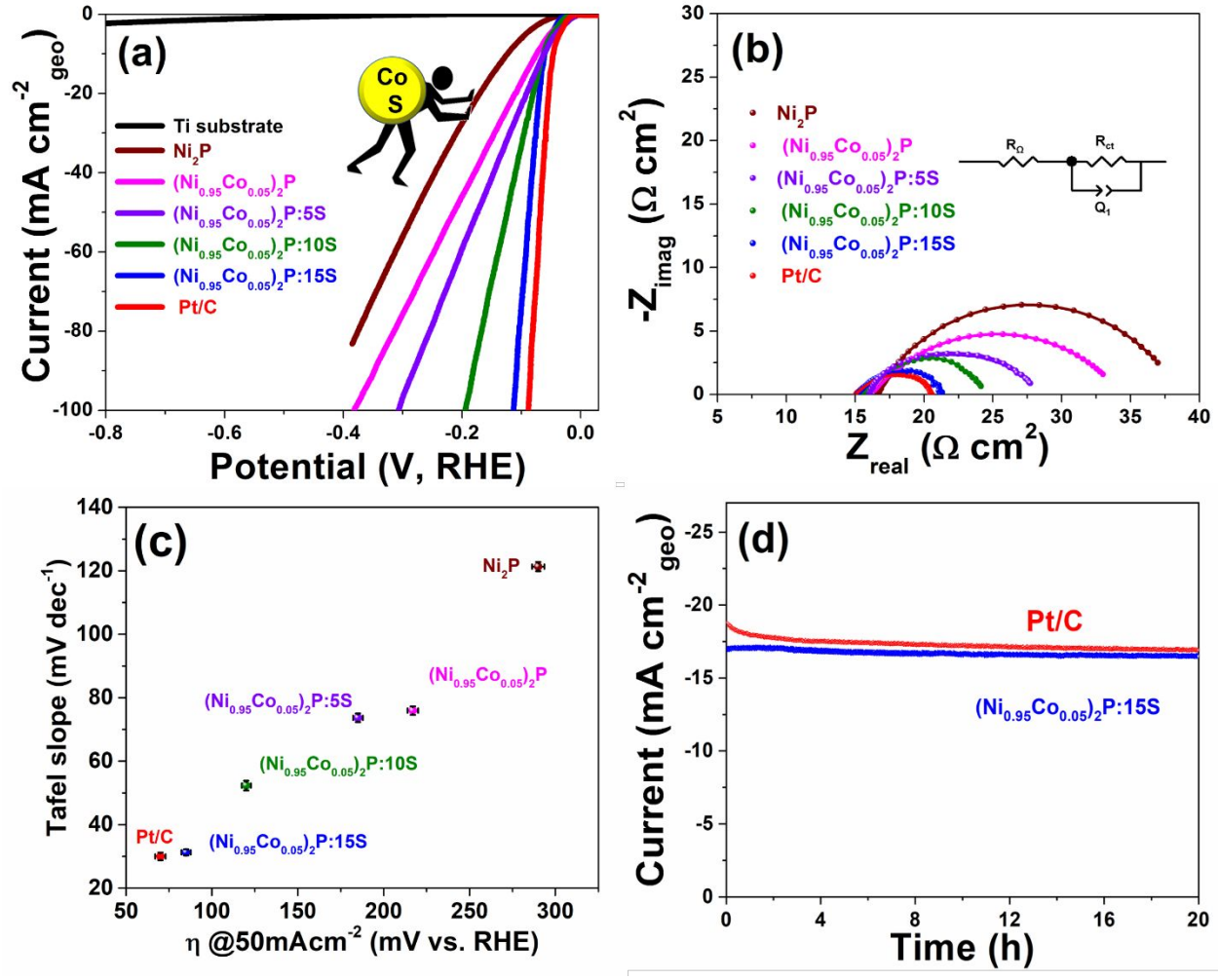

Figure 7. Comparison of electrochemical performances of the as-synthesized electrocatalysts measured in a 1 N H_2SO_4 electrolyte at 40 °C (a) HER polarization (mA cm^{-2}_{geo} *vs.* potential) curves with a scan rate of 10 mVs^{-1}, (b) EIS plots performed at -0.05

V (*vs.* RHE), (c) Tafel slope *vs.* overpotential at 50 mA cm^{-2}_{geo}, and (d) chronoamperometric response of as-prepared Pt/C and $(Ni_{0.95}Co_{0.05})_2P$: 15S electrodes measured at -0.05 V (*vs* RHE).

References

1. P. Di Sia, *J Nanosci Adv Tech*, 2018, **2**, 6-13.
2. P. P. Patel, S. D. Ghadge, P. J. Hanumantha, M. K. Datta, B. Gattu, P. M. Shanthi and P. N. Kumta, *International Journal of Hydrogen Energy*, 2018, **43**, 13158-13176.
3. P. P. Patel, O. I. Velikokhatnyi, S. D. Ghadge, P. J. Hanumantha, M. K. Datta, R. Kuruba, B. Gattu, P. M. Shanthi and P. N. Kumta, *International Journal of Hydrogen Energy*, 2018, **43**, 7855-7871.
4. S. D. Ghadge, O. I. Velikokhatnyi, M. K. Datta, P. M. Shanthi, S. Tan and P. N. Kumta, *ACS Applied Energy Materials*, 2020, **3**, 541-557.
5. S. D. Ghadge, O. I. Velikokhatnyi, M. K. Datta, P. M. Shanthi, S. Tan, K. Damodaran and P. N. Kumta, *ACS Catalysis*, 2019, **9**, 2134-2157.
6. S. D. Ghadge, P. P. Patel, M. K. Datta, O. I. Velikokhatnyi, P. M. Shanthi and P. N. Kumta, *Journal of Power Sources*, 2018, **392**, 139-149.
7. S. D. Ghadge, P. P. Patel, M. K. Datta, O. I. Velikokhatnyi, R. Kuruba, P. M. Shanthi and P. N. Kumta, *RSC Advances*, 2017, **7**, 17311-17324.
8. L. B. Railsback, *Geology*, 2003, **31**, 737-740.

9. M. Mahdi Najafpour, D. Jafarian Sedigh, S. Maedeh Hosseini and I. Zaharieva, *Inorganic chemistry*, 2016, **55**, 8827-8832.

10. J. Luo, J.-H. Im, M. T. Mayer, M. Schreier, M. K. Nazeeruddin, N.-G. Park, S. D. Tilley, H. J. Fan and M. Grätzel, *Science*, 2014, **345**, 1593-1596.

11. Y. Jiao, Y. Zheng, M. Jaroniec and S. Z. Qiao, *Chemical Society Reviews*, 2015, **44**, 2060-2086.

12. P. Xu, J. Zhang, Z. Ye, Y. Liu, T. Cen and D. Yuan, *Applied Surface Science*, 2019, **494**, 749-755.

13. M. A. Khan, H. Zhao, W. Zou, Z. Chen, W. Cao, J. Fang, J. Xu, L. Zhang and J. Zhang, *Electrochemical Energy Reviews*, 2018, **1**, 483-530.

14. P. Xiao, M. A. Sk, L. Thia, X. Ge, R. J. Lim, J.-Y. Wang, K. H. Lim and X. Wang, *Energy & Environmental Science*, 2014, **7**, 2624-2629.

15. P. Liu, J. A. Rodriguez, T. Asakura, J. Gomes and K. Nakamura, *The Journal of Physical Chemistry B*, 2005, **109**, 4575-4583.

16. J. Xiong, J. Li, J. Shi, X. Zhang, N.-T. Suen, Z. Liu, Y. Huang, G. Xu, W. Cai and X. Lei, *ACS Energy Letters*, 2018, **3**, 341-348.

17. B. Hammer and J. K. Nørskov, *Advances in catalysis*, 2000, **45**, 71-129.

18. T. Bligaard and J. K. Nørskov, *Electrochimica Acta*, 2007, **52**, 5512-5516.

19. J. K. Nørskov, T. Bligaard, A. Logadottir, J. Kitchin, J. Chen, S. Pandelov and U. Stimming, *Journal of The Electrochemical Society*, 2005, **152**, J23-J26.

20. R.-K. Chiang and R.-T. Chiang, *Inorganic chemistry*, 2007, **46**, 369-371.

21. R. Fruchart, A. Roger and J. P. Senateur, *Journal of Applied Physics*, 1969, **40**, 1250-1257.

22. Q. Li and X. Hu, *Physical Review B*, 2006, **74**, 035414.

23. Y.-R. Luo, *Comprehensive handbook of chemical bond energies*, CRC press, 2007.

24. Y. Qi, L. Zhang, L. Sun, G. Chen, Q. Luo, H. Xin, J. Peng, Y. Li and F. Ma, *Nanoscale*, 2020, **12**, 1985-1993.

25. J. Lin, Y. Yan, T. Liu, J. Cao, X. Zhou, J. Feng and J. Qi, *International Journal of Hydrogen Energy*, 2020.

26. X. Fang, Z. Wang, Z. Jiang, J. Wang and M. Dong, *Electrochimica Acta*, 2019, **322**, 134739.

27. C. Spoeri, J. T. H. Kwan, A. Bonakdarpour, D. P. Wilkinson and P. Strasser, *Angew. Chem. Int. Ed.*, 2017, **56**, 5994-6021.

28. M. K. Datta, K. Kadakia, O. I. Velikokhatnyi, P. H. Jampani, S. J. Chung, J. A. Poston, A. Manivannan and P. N. Kumta, *Journal of Materials Chemistry A*, 2013, **1**, 4026-4037.

29. H. Zhao, Y. Wang, L. Fang, W. Fu, X. Yang, S. You, P. Luo, H. Zhang and Y. Wang, *Journal of Materials Chemistry A*, 2019, **7**, 20357-20368.

30. H. Ang, H. T. Tan, Z. M. Luo, Y. Zhang, Y. Y. Guo, G. Guo, H. Zhang and Q. Yan, *Small*, 2015, **11**, 6278-6284.

31. H. T. Phan, N. Caney, P. Marty, S. Colasson and J. Gavillet, *International Journal of Heat and Mass Transfer*, 2009, **52**, 5459-5471.

32. Q. Zhang, T. Li, J. Liang, N. Wang, X. Kong, J. Wang, H. Qian, Y. Zhou, F. Liu and C. Wei, *Journal of Materials Chemistry A*, 2018, **6**, 7509-7516.

33. I. I. Abu and K. J. Smith, *Journal of Catalysis*, 2006, **241**, 356-366.

34. H. W. Nesbitt, D. Legrand and G. M. Bancroft, *Physics and Chemistry of Minerals*, 2000, **27**, 357-366.

35. H. Pfeiffer, F. Tancret and T. Brousse, *Electrochimica Acta*, 2005, **50**, 4763-4770.

36. J. Tian, Q. Liu, A. M. Asiri and X. Sun, *Journal of the American Chemical Society*, 2014, **136**, 7587-7590.

37. Y. Teng, A. Wang, X. Li, J. Xie, Y. Wang and Y. Hu, *Journal of Catalysis*, 2009, **266**, 369-379.

38. P. Jiang, Q. Liu, C. Ge, W. Cui, Z. Pu, A. M. Asiri and X. Sun, *Journal of Materials Chemistry A*, 2014, **2**, 14634-14640.

39. A. D. Wilson, R. H. Newell, M. J. McNevin, J. T. Muckerman, M. Rakowski DuBois and D. L. DuBois, *Journal of the American Chemical Society*, 2006, **128**, 358-366.

40. A. D. Wilson, R. K. Shoemaker, A. Miedaner, J. T. Muckerman, D. L. DuBois and M. R. DuBois, *Proceedings of the National Academy of Sciences*, 2007, **104**, 6951-6956.

41. Y. Nicolet, A. L. de Lacey, X. Vernède, V. M. Fernandez, E. C. Hatchikian and J. C. Fontecilla-Camps, *Journal of the American Chemical Society*, 2001, **123**, 1596-1601.

42. J. Chang, K. Li, Z. Wu, J. Ge, C. Liu and W. Xing, *ACS applied materials & interfaces*, 2018, **10**, 26303-26311.

43. X. Cui, Z. Chen, Z. Wang, M. Chen, X. Guo and Z. Zhao, *ACS Applied Energy Materials*, 2018, **1**, 5822-5829.

44. J. Towns, T. Cockerill, M. Dahan, I. Foster, K. Gaither, A. Grimshaw, V. Hazlewood, S. Lathrop, D. Lifka and G. D. Peterson, *Computing in science & engineering*, 2014, **16**, 62-74.

Table of contents

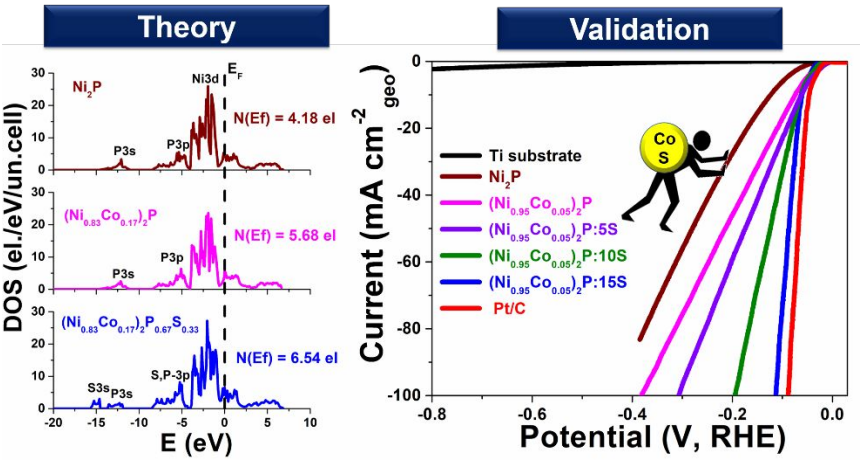

DFT study illuminating modification of the electronic structure and corresponding experimental validation of the enhanced acid mediated HER activity of Co and S doped Ni_2P